Chemical Science

RSC Publishing

EDGE ARTICLE

View Article Online
View Journal | View Issue

Cite this: *Chem. Sci.*, 2013, **4**, 3166

Intramolecular *versus* intermolecular electronic interactions between [5,6]-open and [6,6]-closed C_{60} adducts with exTTF†

Yuta Takano,[ab] Christina Schubert,[c] Naomi Mizorogi,[b] Lai Feng,[bd] Azusa Iwano,[b] Mikimasa Katayama,[b] M. Ángeles Herranz,[e] Dirk M. Guldi,*[c] Nazario Martín,*[ef] Shigeru Nagase*[g] and Takeshi Akasaka*[bhi]

Received 2nd January 2013
Accepted 15th May 2013

DOI: 10.1039/c3sc00004d

www.rsc.org/chemicalscience

Intramolecular and intermolecular electronic interactions are important concepts for fabricating fullerene-based nanostructures such as bulk heterojunction (BHJ) solar cells and supramolecular assemblies. To ascertain differences of the molecular interactions depending on the electronic characteristics of the fullerene adducts, we have synthesized and investigated the [5,6]-open and [6,6]-closed adducts of C_{60}, which are covalently linked to π-extended tetrathiafulvalene (exTTF) by a flexible σ-bond chain. The two adducts were synthesized by means of cycloaddition reactions and were characterized using spectroscopic methods such as MALDI-TOF mass spectrometry and NMR spectroscopy. Electronic properties of the [5,6]-open and [6,6]-closed adducts were investigated in the ground and excited states using steady-state absorption spectroscopy, cyclic and differential pulse voltammetry (CV and DPV), fluorescence spectroscopy, and femtosecond time-resolved absorption spectroscopy. DFT calculations of the two adducts predict that the flexible bridge between C_{60} and exTTF enables a closer proximity than the interlayer distance of graphite (3.35 Å), which dictates considerable π–π interactions. In comparing the [5,6]- and [6,6]-adducts, it is noteworthy to mention that the [6,6]-adduct revealed longer lifetimes of the photochemically formed radical ion pair states than that of the [5,6]-adduct, which is in contrast to results of recent investigations related to the photodynamics of [5,6]- and [6,6]-adducts of C_{60}. Titration experiments using references, namely [5,6]- and [6,6]-$PC_{61}BM$, inferred that the [6,6]-adduct gives rise to stronger electronic interactions with exTTF than the [5,6]-adduct. Comprehensive understanding of the different molecular properties, which the [5,6]- and [6,6]-adducts exhibit, provides valuable information regarding the morphology and/or the electronic properties of C_{60}-based nanocomposites, such as C_{60}-based BHJ solar cells or supramolecular assemblies.

Introduction

Fullerenes are unique molecular carbon materials that are widely used as building blocks for organic photovoltaics (OPV)[1] and for the self-organization of electro- and photoactive components.[2] In this context, the peculiar spherical, three-dimensional molecular structure and the electrochemical as well as the photophysical properties of fullerenes are key incentives.[3] Importantly, the rigid π-conjugated electronic skeleton of fullerenes evokes a remarkably low reorganization energy in electron transfer reactions, enabling charge recombination dynamics in, for example, OPVs in the Marcus inverted region.[4] In addition, π–π interactions, as they take place between the curved π-system of fullerenes and its counterparts, such as

[a]*Institute for Integrated Cell-Material Sciences (WPI-iCeMS), Kyoto University, Sakyo-ku, Kyoto 606-8501, Japan*

[b]*Life Science Center of Tsukuba Advanced Research Alliance, University of Tsukuba, Tsukuba, Ibaraki 305-8577, Japan. E-mail: akasaka@tara.tsukuba.ac.jp*

[c]*Friedrich-Alexander-Universität Erlangen-Nürnberg, Department of Chemistry and Pharmacy & Interdisciplinary Center for Molecular Materials (ICMM), Egerlandstrasse 3, Erlangen 91058, Germany. E-mail: guldi@chemie.uni-erlangen.de*

[d]*Jiangsu Key Laboratory of Thin Films and School of Energy, Soochow University, Suzhou 215006, China*

[e]*Departamento de Química Orgánica I, Facultad de Química, Universidad Complutense, Madrid E-28040, Spain. E-mail: nazmar@quim.ucm.es*

[f]*IMDEA – Nanoscience, Campus de Cantoblanco, Madrid E-28049, Spain*

[g]*Fukui Institute for Fundamental Chemistry, Kyoto University, Sakyo-ku, Kyoto 606-8103, Japan. E-mail: nagase@ims.ac.jp*

[h]*State Key Laboratory of Materials Processing and Die & Mould Technology, School of Materials Science and Technology, Huazhong University of Science and Technology, Wuhan 430074, China*

[i]*Foundation for Advancement of International Science, Tsukuba, Ibaraki 305-0821, Japan*

† Electronic supplementary information (ESI) available: Supporting figures, detailed experimental procedures, and computational methods. See DOI: 10.1039/c3sc00004d

convex buckybowls[5] and concave π-extended tetrathiafulvalene (exTTF), offer myriad opportunities for self-organization.[2]

Chemical functionalization of fullerenes has been employed to gain control over the physical properties of fullerenes in the search for practical applications.[3] To this end, [6,6]-phenyl-C_{61}-butyric acid methyl ester ([6,6]-$PC_{61}BM$) is a thoroughly studied fullerene derivative, especially in the area of photovoltaic applications. It is primarily the outstanding electrochemical and photophysical properties of [6,6]-$PC_{61}BM$ that make the difference.[1,6] Likewise, an easy processability renders [6,6]-$PC_{61}BM$ ideally suited for device fabrication.

Among the different fullerene adducts, the [5,6]-open and [6,6]-closed adducts, so-called [5,6]-fulleroids and [6,6]-methanofullerenes, have been shown to feature different electronic properties. For instance, [5,6]-fulleroids are considered as 60 π-electron systems virtually similar to pristine C_{60}. In contrast, [6,6]-methanofullerenes have a 58 π-electron system, in which two π-electrons are lost as a result of chemical functionalization and, in turn, leading to a loss of conjugation. Fundamental properties including intermolecular and intramolecular electron transfer reactions provide important guidelines for the fabrication of molecular devices. They remain, however, limited by the scarce number of reports dealing with the different behaviour of C_{60} adducts, that is, a direct comparison between the different [5,6]-open *versus* [6,6]-closed fullerene cycloadducts.

We have previously reported the photodynamics in C_{60}–exTTF electron donor–acceptor conjugates linked in either a [5,6]-open or [6,6]-closed fashion.[7] Importantly, in these conjugates, exTTF is rigidly fixed to fulleropyrrolidine and charge separation as well as charge recombination dynamics are nearly comparable between the [5,6]-open (*i.e.*, 104 ps *versus* 150 ns in CH_2Cl_2) and [6,6]-closed (*i.e.*, 113 ps *versus* 110 ns in CH_2Cl_2) isomers.

In the current contribution, we describe the synthesis and characterization of a new class of electron donor–acceptor conjugates in which an electron donating exTTF has been covalently linked to a [5,6]-open (**3a**) and a [6,6]-closed (**3b**) C_{60} through a flexible σ-bond chain. Remarkably, the charge separation and charge recombination dynamics differ significantly between the [5,6]-open (**3a**) and [6,6]-closed (**3b**) isomers. This is in sharp contrast to the dynamics previously reported for C_{60}–exTTF conjugates, in which the two electro- and photoactive moieties are rigidly connected.

Results and discussion

The syntheses of **3a** and **3b** were conducted by means of cycloaddition reactions of exTTF–diazo compounds that had been prepared *in situ* by a Bamford–Stevens reaction between exTTF–tosylhydrazone (**2**) and sodium methoxide (Scheme 1). The thermal reaction of C_{60} with **2** at 75 °C gave mainly rise to the [5,6]-open isomer of C_{60}–exTTF (**3a**), which was detected using HPLC analysis (Fig. 1). The [6,6]-closed adduct (**3b**) was obtained using the thermal conversion of **3a** by heating in refluxing toluene for 10 h without severe decomposition (Fig. S1, see ESI†). This result is consistent with the fact that generally [5,6]-open adducts are kinetic products and [6,6]-closed adducts are thermodynamic products in cycloadducts of C_{60}.[6] **3a** and **3b** were respectively isolated and purified using HPLC (Fig. S2†).

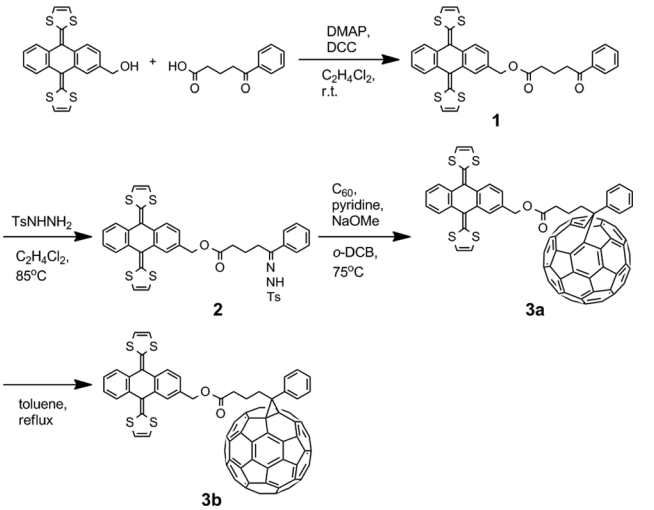

Scheme 1 Synthesis of [5,6]-open exTTF–C_{60} **3a** and [6,6]-closed exTTF–C_{60} **3b**.

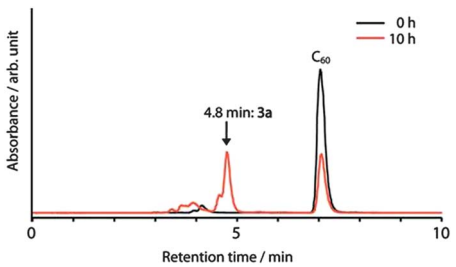

Fig. 1 HPLC profile of the reaction mixture of **3**: column, Buckyprep ϕ 4.6 × 250 mm; flow rate, 1.0 mL min^{-1}; wavelength, 330 nm; eluent, toluene; temperature, r.t.

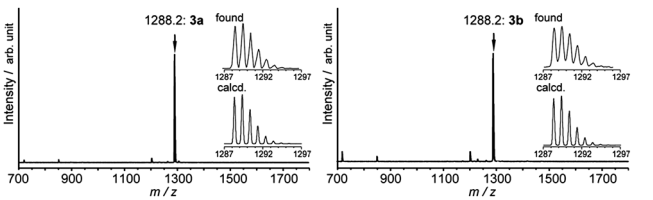

Fig. 2 MALDI-TOF mass spectra of isolated **3a** (left) and **3b** (right) in negative ion mode.

MALDI-TOF mass spectra provided structural information about **3a** and **3b**, which show the expected molecular ion peaks at 1288 *m*/*z* (Fig. 2).

^{1}H-NMR spectra of **3a** and **3b** showed characteristic signals of the organic addend, that is, the exTTF moiety tethered to C_{60} (Fig. 3). The resonances for the aromatic protons of the anthracene group in the exTTF moiety appear between 7.7 and 7.2 ppm, while the signals of the two 1,3-dithiole rings appear in the region around 6.3 ppm for **3a** and **3b**. Assignments of all signals were achieved by the combination of 1D and 2D NMR techniques including H–H COSY, HMQC, and HMBC spectra (see ESI†).

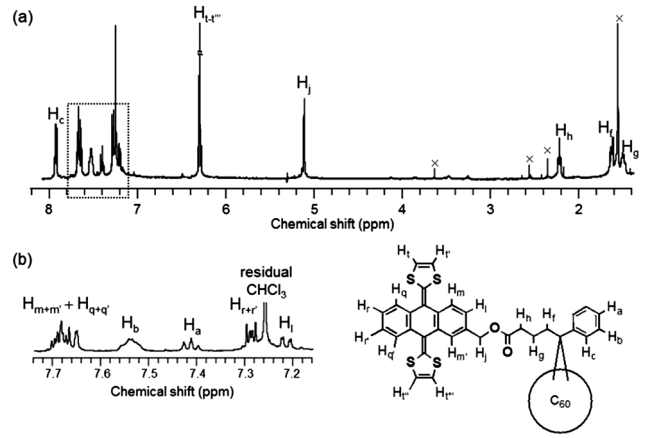

Fig. 3 Upper part: ^{1}H NMR signals and their assignments of **3a** at 300 MHz in $CDCl_3$. Lower part: expansion of the aromatic region.

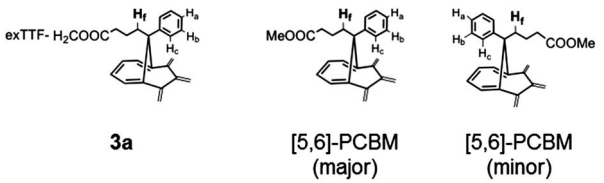

Fig. 4 Schematic drawing of **3a** and the two possible regioisomers of [5,6]-open adducts of $PC_{61}BM$ (**4a**).

Table 1 Proton peaks of ^{1}H NMR spectra of **3a** and [5,6]-$PC_{61}BM$ isomers in $CDCl_3$

Compound	H_a (ppm)	H_b (ppm)	H_c (ppm)	H_f (ppm)
3a	7.41	7.52–7.56	7.93	1.62–1.65
[5,6]-$PC_{61}BM$ (major)[a]	7.37	7.50	7.87	1.58
[5,6]-$PC_{61}BM$ (minor)[a]	7.10	7.19	7.01	3.78

[a] Data from ref. 6.

^{13}C NMR spectra of **3a** and **3b** show signals from C_{60} and the organic addend, including exTTF (Fig. S8 and S14†). Thus, **3a** and **3b** show 32 signals from C_{60}, clearly showing the C_s molecular symmetry of both compounds. On the other hand, a significant difference between **3a** and **3b** was observed in the signals that stem from the bridgehead carbon atoms of C_{60} at 139.6 pm for **3a** and at 79.3 ppm for **3b**. These results verify that **3a** and **3b** are [5,6]-open and [6,6]-closed adducts, respectively, as they reflect the sp^2 and sp^3 character.

Although two regioisomers are formed for the [5,6]-open adduct **3a** (Fig. 4), only one isomer was detected and isolated in a one-step HPLC purification. From the trends in the chemical shifts between **3a** and the previously reported [5,6]-$PC_{61}BM$, we

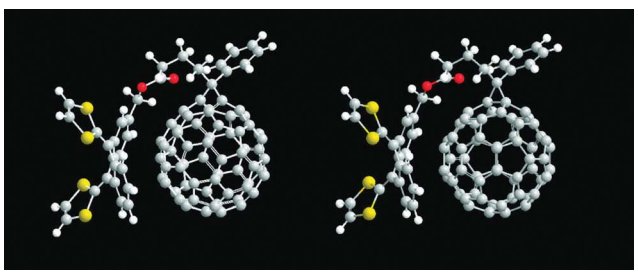

Fig. 5 Optimized structures of **3a** (left) and **3b** (right) calculated at the M06-2X/6-31 G(d) level of theory. Carbon, hydrogen, oxygen, and sulfur atoms are coloured in grey, white, red, and yellow, respectively. **3b** is 13.8 kcal mol^{-1} more stable than **3a**. Other possible conformers are shown in Fig. S19 in ESI.†

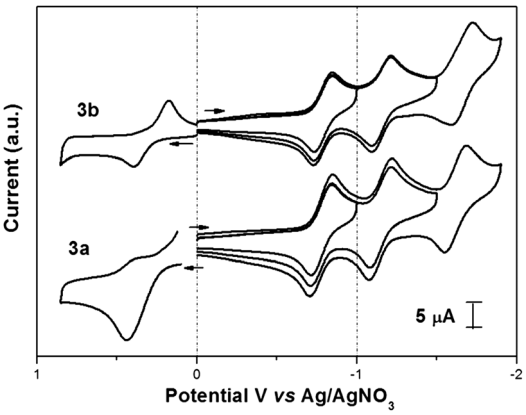

Fig. 6 CV of **3a** and **3b** measured in *o*-dichlorobenzene at room temperature.

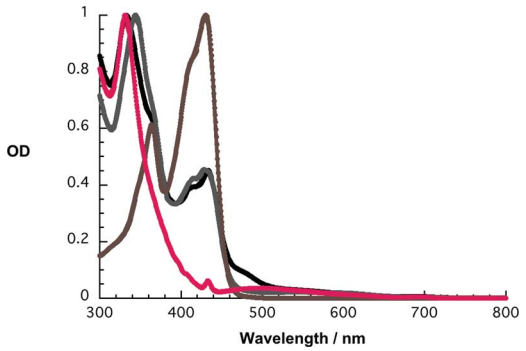

Fig. 7 Room temperature absorption spectra of [6,6]-closed exTTF–C_{60} **3b** (black spectrum) and [5,6]-open exTTF–C_{60} **3a** (grey spectrum) in toluene along with those of exTTF (brown spectrum) and [6,6]-$PC_{61}BM$ (**4b**) (red spectrum).

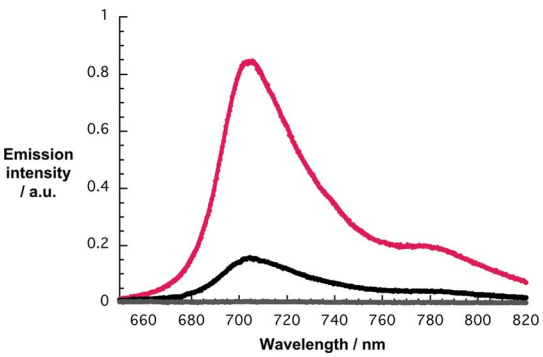

Fig. 8 Room temperature fluorescence spectra of [6,6]-closed exTTF–C_{60} **3b** (black spectrum), [5,6]-open exTTF–C_{60} **3a** (grey spectrum), and [6,6]-$PC_{61}BM$ **4b** (red spectrum) in toluene with matching absorption at the 340 nm excitation wavelength, $OD_{340nm} = 0.1$.

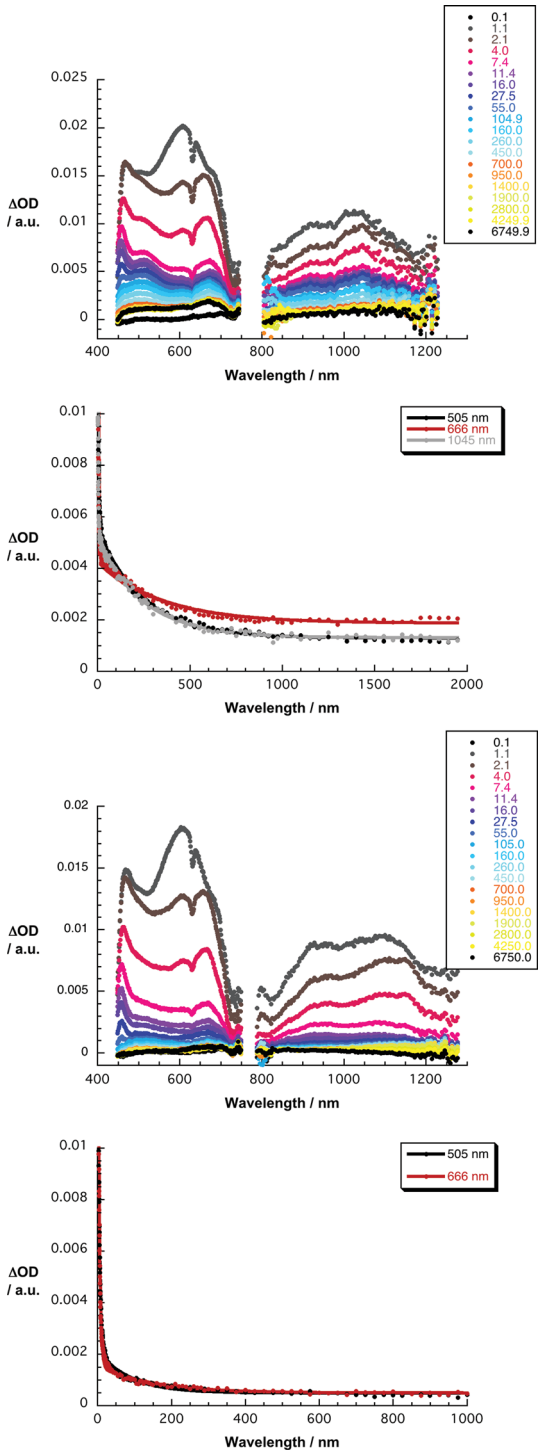

Fig. 9 Upper part: differential absorption spectra (visible and near-infrared) obtained upon femtosecond flash photolysis (387 nm, 200 nJ) of [6,6]-closed exTTF–C_{60} **3b** in argon-saturated THF with time delays between 0.1 and 6750 ps at room temperature. Upper central part: time-absorption profiles at 505, 666, and 1045 nm monitoring the charge separation and charge recombination dynamics. Lower central part: differential absorption spectra (visible and near-infrared) obtained upon femtosecond flash photolysis (387 nm, 200 nJ) of [5,6]-open exTTF–C_{60} **3a** in argon-saturated THF with time delays between 0.1 and 6750 ps at room temperature. Lower part: time-absorption profiles at 505 and 666, nm monitoring the charge separation and charge recombination dynamics.

conclude that **3a** has the same bonding pattern as the major isomer of [5,6]-$PC_{61}BM$ (**4a**), in which the phenyl ring situates on top of the pentagon ring (Table 1).[6]

Additional information related to the molecular structures was provided by theoretical calculations of **3a** and **3b** using DFT at the M06-2X[8]/6-31 G(d) level[9] with a Gaussian 09 package.[10] Fig. 5 and S19† show optimized structures of **3a** and **3b**, and their corresponding energy-minimum conformers. It is worth mentioning that the distance between C_{60} and exTTF tends to be rather short in **3a** and **3b**. In fact, the bridge avoids stretching. The shortest intramolecular distances (3.29 Å for **3a**; 3.25 Å for **3b**) are shorter than the interlayer distance of graphite (3.35 Å)[11] and closer than that between two benzenes in a solution dimer (3.49 Å),[12] which prompts to considerable through–space interactions, even though real molecular configurations of **3a** and **3b** in a solution system might not be completely the same. In addition, DFT calculations predict that **3a** and **3b** exhibit similar MO distributions with the LUMO localized on C_{60} and the HOMO spreading over exTTF (Fig. S20†).

The electrochemical properties of **3a** and **3b** were investigated using differential pulse voltammetry (DPV) and cyclic voltammetry (CV) (Fig. 6, Table S1†). Using exTTF, [6,6]-closed $PC_{61}BM$ (**4b**), and C_{60} as references enables the accurate assignment of the individual redox steps. In **3a** and **3b**, the first oxidation is attributed to the formation of the dicationic exTTF, which involves a quasi-reversible two-electron oxidation step. The C_{60}–exTTF adducts display three quasi-reversible reduction peaks in the investigated solvent window. Overall, there is essentially no difference in the reduction potentials of the two isomers, which exhibit a decreased electron affinity when compared with C_{60} by *ca.* 70–80 mV. The effect of the π electron count on the reduction potentials of the two isomers is along the lines of the investigations previously reported on [5,6]-open and [6,6]-closed adducts.[13] The band gap estimated from the electrochemical measurements lays between 1.18 ± 0.04 V, which is in agreement with the comparable energy calculated for the HOMO and LUMO levels of both systems (Fig. S20†).

Upon closer analysis of the absorption spectra measured in toluene, the [6,6]-closed and [5,6]-open isomers reveal distinct differences (Fig. 7). For example, the [6,6]-closed reference – **4b**– and **3b** both show the fundamentally important 0–0 transition at 700 nm, which originates from monofunctionalization of C_{60} and which reflects their partially broken symmetry (C_s) relative to pristine C_{60} (I_h). The C_{60} centered band at 430 nm is masked by the much stronger exTTF absorption in this range. Importantly, the absorption spectrum of **3a** lacks this particular feature. In addition, the 330 nm maximum is bathochromically shifted to 344 nm when compared to **4b** and **4a**. These results corroborate that the 60 π-electron nature of C_{60} is mostly preserved in **3a**. In other words, **3a** is isoelectronic with pristine C_{60}.

Preliminary insights into excited state interactions came from steady-state fluorescence experiments (Fig. 8). To ensure almost exclusive excitation of C_{60}, 340 nm was selected as the excitation wavelength. In **3a** and **3b**, a notable fluorescence quenching is discernible in comparison to **4b**.[14] In fact, the underlying fluorescence quantum yields gave rise to two appreciable trends. Firstly, changing the solvent from non-polar toluene ($\varepsilon = 2.4$) to

medium-polar THF ($\varepsilon = 7.6$) results in a gradual intensification of fluorescence quenching with quantum yields of 1.8×10^{-4} and 3.9×10^{-5}. Secondly, **3a** is susceptible to stronger fluorescence quenching ($<3 \times 10^{-5}$) than **3b**.

Excited state interactions in **3a** and **3b** were elucidated using information from femtosecond transient absorption experiments, as presented in Fig. 9. Following 387 nm excitation, the instantaneous formation of the C_{60} and exTTF singlet excited states with their 918 and 600 nm maxima is seen to evolve. In contrast to what is, however, seen for the references, that is, [6,6]-$PC_{61}BM$ (**4b**) and exTTF, the singlet excited state decays in the [5,6]-open and [6,6]-closed C_{60}–exTTFs rather quickly. A likely mechanism for the deactivation is an intramolecular charge transfer to yield an intramolecular radical ion pair state. In the visible range, it is important to note that the newly developing maximum at 660 nm closely resembles the spectral feature of the radical cation of exTTF.[15] In the near-infrared range, the radical anion absorptions of C_{60}, which differ for the [6,6]-closed[16] and the [5,6]-open,[7] evolve at 1040 and 1100 nm, respectively. Kinetic analyses suggest that [5,6]-open C_{60}–exTTF reacts faster in terms of charge separation and charge recombination than [6,6]-closed C_{60}–exTTF. For example, charge separation in THF occurs within 1 ps for [5,6]-open C_{60}–exTTF and 3 ps for [6,6]-closed C_{60}–exTTF. When turning to charge recombination in THF, values of 18 and 270 ps are derived for the [5,6]-open and [6,6]-closed C_{60}–exTTFs, respectively. It is likely that the difference in charge recombination relates to the different π-electron system in the [5,6]-open (60 π electrons) and [6,6]-closed (58 π electrons) isomers and the different junctions in the [5,6]-open (sp^2 hybridized carbon) and [6,6]-closed (sp^3 hybridized carbon) isomers, besides the slightly different driving force.

In general, a trend evolves for the charge recombination that implies 10 times longer lived radical ion pair states for the [6,6]-closed isomer than for the [5,6]-open isomer. Additional support for this notion came from an increase in solvent polarity (*i.e.*, DMF) and a decrease (*i.e.*, toluene). This is meant to decrease the thermodynamic driving force for charge recombination in the earlier case or to increase it in the latter case. In DMF the lifetimes are 11 and 200 ps, while in toluene the respective lifetimes are 51 and 560 ps for [5,6]-open and [6,6]-closed C_{60}–exTTFs, respectively. In contrast to recent investigations, our current data indicate charge recombination dynamics that are placed deeply into the inverted region of the Marcus parabola.

Owing to the flexibility of the linker that connects C_{60} and exTTF free rotation around the single bonds is likely to happen. In fact, we must assume that in the [5,6]-open and [6,6]-closed C_{60}–exTTFs C_{60} and exTTF adopt a conformation that allows close proximity, namely π–π interactions.[17] In this particular case, any charge transfer – charge separation and charge recombination – are governed by a through space mechanism. Critically they are solely the relative proximity and the extent of molecular overlap.

In terms of general properties, the solubility of **3b** is markedly lower than that of **3a** in solvents such as toluene, $CHCl_3$, and CS_2. Overall, the lower solubility is attributable to the difference in the intramolecular and intermolecular interaction between exTTF and the [5,6]-open or [6,6]-closed isomers of C_{60}, which might eventually lead to aggregation *etc.* This hypothesis was corroborated through titration experiments employing absorption spectroscopy. Titrating, for example, exTTF–OH with **4b** results in characteristic changes in the absorption, especially around 480 nm, which suggests charge transfer interactions evolving between exTTF and C_{60} (Fig. 10).[18] ExTTF and **4a** failed to give rise to any appreciable changes when the same concentrations were used. From these results it is safe to infer that exTTF interacts *intermolecularly* stronger with the [6,6]-closed isomer than with the [5,6]-open isomer. We believe that this result is directly applicable to **3a** and **3b**, in which exTTF may reach the surface of C_{60} rather freely owing to the flexible linkage. As such, intermolecular interactions between exTTF and C_{60} are expected to be stronger in **3b** than in **3a**. Consequently, these favoured intermolecular interactions in **3b** may lead to a lower solubility than in **3a**. Furthermore, they can also play a major role in the stabilization of the radical ion pair state of the [6,6]-open isomer generated after photoexcitation, which would result in a slower charge recombination.

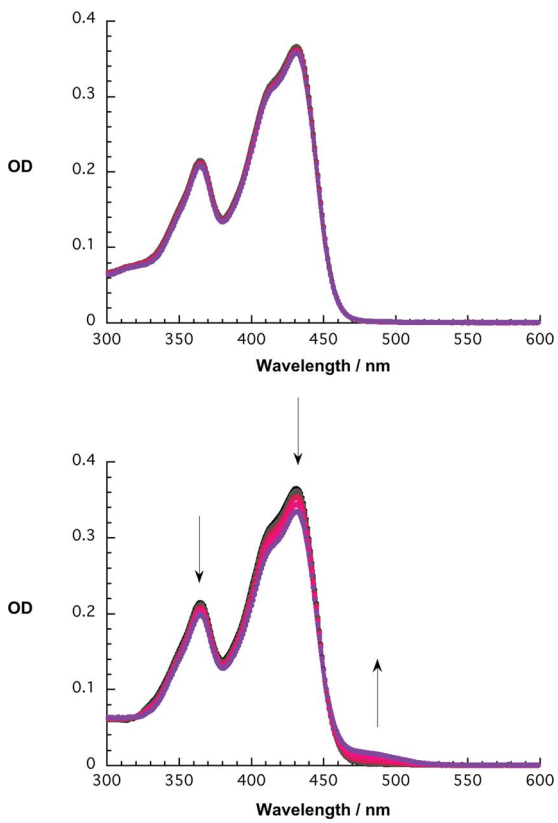

Fig. 10 Upper part: room temperature absorption spectra upon titrating exTTF–OH with **4a**. Lower part: room temperature absorption spectra upon titrating exTTF–OH with **4b**. Arrows indicate the changes in absorption due to interactions between exTTF–OH and C_{60}.

Conclusions

Novel electron donor–bridge–acceptor conjugates involving exTTF and C_{60}, respectively, revealed a remarkable difference between the corresponding [5,6]-open (**3a**) and [6,6]-closed (**3b**) adducts in their excited state. Such behaviour, although the

[5,6]-open monoadduct reveals a slightly better acceptor ability and a stronger quenching of the fluorescence in steady-state experiments, is ascribed to the difference in excited state energies of the two isomers, that is, [5,6]-open and [6,6]-closed, and the lower photostability of the [5,6]-open isomer.[19] DFT calculations predict that the flexible bridge that links C_{60} and exTTF enables a close proximity between the two electro- and photoactive constituents through π–π interactions. Interestingly, and in contrast to previous reports, [6,6]-closed C_{60}–exTTF (**3b**) features longer lifetimes of the radical ion pair state when compared to [5,6]-open C_{60}–exTTF (**3a**). The different π-electron system in the [5,6]-open (60 π electrons) and [6,6]-closed (58 π electrons) isomers and the different junctions in the [5,6]-open (sp^2 hybridized carbon) and [6,6]-closed (sp^3 hybridized carbon) isomers are believed to impact the lifetimes. As such, our current results provide ample information regarding electron transfer processes involving [6,6]-closed and [5,6]-open isomers.

Acknowledgements

This work was supported in part by a Grant-in-Aid for Scientific Research on Innovative Areas (no. 20108001, "pi-Space"), a Grant-in-Aid for Scientific Research (A) (no. 20245006) and (B) (no. 24350019), The Next Generation Super Computing Project (Nanoscience Project), Nanotechnology Support Project, a Grant-in-Aid for Scientific Research on Priority Area (no. 20036008, 20038007), and Specially Promoted Research from the Ministry of Education, Culture, Sports, Science, and Technology of Japan and The Strategic Japanese–Spanish Cooperative Program funded by JST and MINECO (Projects PLE-2009-0039 and PIB2010JP-00196). The iCeMS is supported by World Premier International Research Center Initiative (WPI), MEXT, Japan. This work was also supported in part by the Deutsche Forschungsgemeinschaft, Cluster of Excellence "Engineering of Advanced Materials", the Bavarian initiative "Solar Technologies go Hybrid", FCI, the Office of Basic Energy Sciences of the U. S. Financial support was also provided by the MINECO of Spain (Projects CTQ2011-24652 and Consolider-Ingenio 2010C-07–25200) and CAM (MADRISOLAR Project P-PPQ-000225-0505).

Notes and references

1 For recent reviews on fullerene-based OPVs, see: (*a*) S. Gunes, H. Neugebauer and N. S. Sariciftci, *Chem. Rev.*, 2007, **107**, 1324–1338; (*b*) B. C. Thompson and J. M. J. Frechet, *Angew. Chem., Int. Ed.*, 2008, **47**, 58–77; (*c*) G. Dennler, M. C. Scharber and C. J. Brabec, *Adv. Mater.*, 2009, **21**, 1323–1338; (*d*) H. Imahori and T. Umeyama, *J. Phys. Chem. C*, 2009, **113**, 9029–9039; (*e*) B. Kippelen and J. L. Bredas, *Energy Environ. Sci.*, 2009, **2**, 251–261; (*f*) J. L. Delgado, P.-A. Bouit, S. Filippone, M. A. Herranz and N. Martín, *Chem. Commun.*, 2010, **46**, 4853–4865.

2 For recent reviews on fullerene-based supramolecular chemistry, see: (*a*) U. Hahn, F. Cardinali and J. F. Nierengarten, *New J. Chem.*, 2007, **31**, 1128–1138; (*b*) K. Tashiro and T. Aida, *Chem. Soc. Rev.*, 2007, **36**, 189–197; (*c*) E. M. Pérez and N. Martín, *Chem. Soc. Rev.*, 2008, **37**, 1512–1519; (*d*) F. D'Souza and O. Ito, *Chem. Commun.*, 2009, 4913–4928; (*e*) E. M. Perez, B. M. Illescas, M. A. Herranz and N. Martín, *New J. Chem.*, 2009, **33**, 228–234; (*f*) F. Giacalone and N. Martín, *Adv. Mater.*, 2010, **22**, 4220–4248; (*g*) D. Canevet, E. M. Pérez and N. Martín, *Angew. Chem., Int. Ed.*, 2011, **50**, 9248–9259; (*h*) D. M. Guldi, *Chem. Commun.*, 2000, 321–327; (*i*) D. M. Guldi, *Chem. Soc. Rev.*, 2002, **31**, 22–36; (*j*) D. M. Guldi, F. Zerbetto, V. Georgakilas and M. Prato, *Acc. Chem. Res.*, 2005, **38**, 38–43.

3 (*a*) *Fullerenes: From Synthesis to Optoelectronic Properties*, ed. D. M. Guldi and N. Martín, Kluver Academic Publishers, Dordrecht, The Netherlands, 2002; (*b*) A. Hirsch and M. Bettreich, *Fullerenes, Chemistry and Reaction*, Wiley-VCH, Weinheim, Germany, 2005; (*c*) *Fullerenes. Principles and Applications*, ed. F. Langa De La Puente and J.-F. Nierengarten, The Royal Society of Chemistry, Cambridge, 2007.

4 (*a*) S. Fukuzumi, K. Ohkubo, H. Imahori, J. G. Shao, Z. P. Ou, G. Zheng, Y. H. Chen, R. K. Pandey, M. Fujitsuka, O. Ito and K. M. Kadish, *J. Am. Chem. Soc.*, 2001, **123**, 10676–10683; (*b*) D. M. Guldi and K.-D. Asmus, *J. Am. Chem. Soc.*, 1997, **119**, 5744–5745.

5 (*a*) A. Sygula, *Eur. J. Org. Chem.*, 2011, 1611–1625; (*b*) S. Higashibayashi and H. Sakurai, *Chem. Lett.*, 2011, **40**, 122–128.

6 J. C. Hummelen, B. W. Knight, F. Lepeq, F. Wudl, J. Yao and C. L. Wilkins, *J. Org. Chem.*, 1995, **60**, 532–538.

7 N. Martín, L. Sánchez and D. M. Guldi, *Chem. Commun.*, 2000, 113–114.

8 Y. Zhao and D. G. Truhlar, *Theor. Chem. Acc.*, 2008, **120**, 215–241.

9 (*a*) R. Ditchfie, W. J. Hehre and J. A. Pople, *J. Chem. Phys.*, 1971, **54**, 724–728; (*b*) W. J. Hehre, R. Ditchfie and J. A. Pople, *J. Chem. Phys.*, 1972, **56**, 2257–2261.

10 M. J. Frisch, *et al.*, *GAUSSIAN 09, Revision A.02*, Gaussian, Inc., Wallingford CT, 2009.

11 Y. Baskin and L. Meyer, *Phys. Rev.*, 1955, **100**, 544.

12 (*a*) E. A. Meyer, R. K. Castellano and F. Diederich, *Angew. Chem., Int. Ed.*, 2003, **42**, 1210–1250; (*b*) S. Grimme, *Angew. Chem., Int. Ed.*, 2008, **47**, 3430–3434.

13 F. Arias, L. Echegoyen, S. R. Wilson, Q. Lu and Q. Lu, *J. Am. Chem. Soc.*, 1995, **117**, 1422–1427.

14 H. Wang, Y. J. He, Y. F. Li and H. M. Su, *J. Phys. Chem. A*, 2012, **116**, 255–262.

15 D. M. Guldi, L. Sánchez and N. Martín, *J. Phys. Chem. B*, 2001, **105**, 7139–7144.

16 D. M. Guldi, H. Hungerbuhler and K. D. Asmus, *J. Phys. Chem.*, 1995, **99**, 9380–9385.

17 (*a*) E. M. Pérez, A. L. Capodilupo, G. Fernández, L. Sánchez, P. M. Viruela, R. Viruela, E. Ortí, M. Bietti and N. Martín, *Chem. Commun.*, 2008, 4567–4569; (*b*) H. Isla, M. Gallego, E. M. Pérez, R. Viruela, E. Ortí and N. Martín, *J. Am. Chem. Soc.*, 2010, **132**, 1772–1773; (*c*) B. Grimm, J. Santos, B. M. Illescas, A. Muñoz, D. M. Guldi and N. Martín, *J. Am. Chem. Soc.*, 2010, **132**, 17387–17389.

18 E. M. Pérez, L. Sánchez, G. Fernández and N. Martín, *J. Am. Chem. Soc.*, 2006, **128**, 7172–7173.

19 D. M. Guldi, H. Hungerbühler, I. Carmichael, K.-D. Asmus and M. Maggini, *J. Phys. Chem. A*, 2000, **104**, 8601–8608.